FDTD Analysis of Retinal Photoreceptor Outer-Segment: Effect of Stacking Nano-Layers of Membrane and Cytoplasm

Amir Hajiaboli[1], *Milica Popović*[1]

[1]Depertment of Electrical and Computer Engineering, McGill University
3480 University Street, Montreal, Quebec H3A 2A7

[1]amir.hajiaboli@mail.mcgill.ca, milica.popovich@mcgill.ca

Abstract

This paper presents finite-difference time-domain (FDTD) analysis of the retinal photoreceptor outer-segment. Our model simulates, in an optical sense, the reaction of the photoreceptor to the visible light spectrum. We consider a broadband pulse excitation to examine the mode coupling. Our investigations include the variations of Poynting power versus wavelength at exiting cross-sections of the outer-segment, and for varying incident angles of the impinging wave. In order to study the role of the stacking nano-layers of the cytoplasm and membrane which comprise the inner photoreceptor anatomy, the results are compared with those obtained from an averaged-permittivity model of the outer-segment.

1. Introduction

In 1963, Enoch's observation of characteristic modal patterns proved that the human photoreceptors are, indeed, optical waveguides and they are capable of funneling and guiding light [1]. Later in 1973, and based on the available physiological data at the time, Snyder and Pask proposed an optical fiber model of the photoreceptor [2]. They exploited the analytical solution of wave propagation and their results successfully revealed some aspects of directional sensitivity in human vision known as the Stiles-Crawford effect of the first kind.

For the waveguide model to be valid, a finite aperture, which limits the bundle of light entering the photoreceptor, is required [3]. However, this may not be a plausible assumption because the diameter of the focused light on the retina is several times larger than the entrance aperture of the photoreceptor [4]. Moreover, the existence of several scattering objects along the light path can diffract the light reaching the photoreceptor. Considering these facts, we here propose a model of the photoreceptor outer-segment, similar to that of a dielectric resonator antenna [5], in which light incident from all directions can enter and propagate within the photoreceptor.

The numerical tool chosen in our work is the finite-difference time-domain(FDTD) method, because of its flexibility in modeling the heterogeneous medium required to model the detail morphology of living cells, such as photoreceptors [6, 7]. Although researchers have been mostly limited to 2-dimensional FDTD formulation due to the computational burden of 3-dimensional simulations, the results have provided a good insight into the problem of light propagation in the retinal rods and cones. For example, in [5], researchers have been able to model the Stiles-Crawford effect through the FDTD simulations.

As the outer-segment of the human photoreceptor is the site of the photon transduction to an electrical signal, we suspect that the detailed morphology of the outer-segment can alter the spectral sensitivity of the photoreceptor. To investigate this, we have calculated and compared the spectrum of light guided by different models of the photoreceptor outer-segment for varying angles of incident light.

2. Model of Photoreceptor Outer-Segment

The outer-segment consists of stacking nano-layers of cytoplasm and folded membrane. The thickness of the layers is much smaller than the light wavelength, so it is plausible, in the waveguide model, to consider them as geometries of a uniform, averaged refractive index [2]. However, when the angle of incidence is not normal to the outer-segment aperture, the presence of these stacking nano-layers can introduce a significant effect. To explore this phenomenon, we compare the results obtained from a model that consists of stacking nano-layers of cytoplasm and membrane and a model which consists of a bulk, permittivity-averaged model.

Previously, we have presented a precise model of the outer-segment including the stacking layers of cytoplasm and membrane [8, 9]. It consists of very thin (~15nm) stacked disks of different refractive index that alternates in value between that of the cytoplasm and that of the folded cell membrane. For relative permittivity, the values of accepted physiological data [3, 6], for the cytoplasm $\varepsilon_{\text{r-cytoplasm}}$=1.85, the membrane $\varepsilon_{\text{r-membrane}}$=2.22 and the intercellular medium

$\varepsilon_{r\text{-intercellular}}$ =1.79 have been adopted. Due to bleaching of the rhodopsin molecules, the refractive index can change over time [10], and to account for this fact, we choose the membrane refractive index in accordance with the physiological data for the dark-adapted and unbleached photoreceptors [11, 12]. Furthermore, as discussed in [13], it is safe to neglect the effects of dispersion. Therefore, we have considered a constant electric loss of $\sigma_{membrane}$=37.38 S/m [11] over the spectrum of visible light. The length of the outer-segment (6.75μm) is, approximately, that of the reported length of the peripheral cones [7].

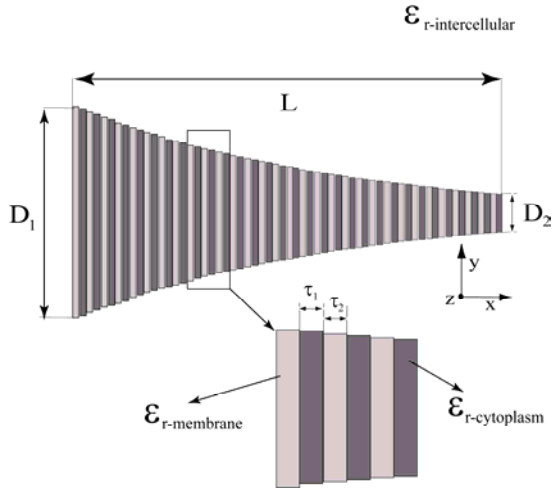

(a)

Fig. 1: a) Model of the geometry of the cone outer-segment. In our study, L=6.75μm and D_1=4.1μm, while D_2 is a variable parameter. The structure consists of very thin (~15nm) alternating stacked layers of different relative permittivity values. For the cytoplasm, τ_1=15nm, $\varepsilon_{r\text{-cytoplasm}}$=1.85; for the folded membrane, τ_2=15nm, $\varepsilon_{r\text{-membrane}}$=2.22 $\sigma_{membrane}$=37.38; for the medium surrounding the outer-segment, $\varepsilon_{r\text{-intercellular}}$=1.79 [4, 6].

In the averaged bulk model the average value of refractive indices of cytoplasm and membrane has been considered.

3. FDTD Simulation Parameters

The geometry is modeled by a uniform FDTD space with Δx=5nm and Δy=Δz=50nm. This discretization results in a total of 1600×140×140=31.36 million FDTD cells. The time-step, based on the Courant-stability condition, is set to Δt=1.49×10^{-2}fs. The incident signal is a y-polarized plane wave propagating in the x-direction, and it is a sinusoid-modulated wideband Gaussian pulse centered at 622THz :

$$E_y = Ae^{-\frac{(t-t_0)^2}{2\sigma^2}} \sin(2\pi f(t-t_0)) \quad (1)$$

Here, A=1V/m is the amplitude of the signal, σ=100Δt is the mean variation of the signal, t_0=400Δt is the delay introduced to preserve the causality of the signal and f=622THz is the frequency of the modulation signal (the region of visible light, λ=482nm). The peak value of the incident field is 125V/m, centered at λ=482nm. The full width at half maximum (FWHM) of the incident plane wave is 250nm and, this covers the required bandwidth to properly model the white light spectrum.

In our work, we adopt the total-field/scattered-field (TF/SF) formulation, which allows us to examine the amount of electromagnetic power coupled into and guided by the outer-segment. Fig. 2 shows the illumination of outer-segment by a plane wave. $\hat{k}_{inc}$ is the incident k-vector and $\hat{E}_{inc}$ represents the polarization vector. Φ is the angle of incidence relative to the x-axis and ψ is the polarization angle based on the model discussed in [14].

As discussed in [15], the electric field parallel to the membrane surface will yield maximal power absorption. Consequently, in our work, we choose ψ=π/2 to ensure that a constant value of the component of the electric field parallel to the membrane, independent of the incident angle, is considered in our simulations.

The forward-scattered fields of E_y, E_z, H_y and H_z on S_F surface shown in Fig. 2 have been sampled at each time step. After applying the Fourier-transform, the time-average Poynting power (S_x) versus frequency has been calculated using the following equation:

$$S_x = Real\{E_y H_z - E_z H_y\} \tag{2}$$

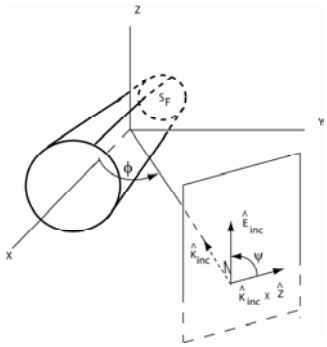

Fig. 2: Outer-segment illuminated by a plane wave.

4. Results and Discussion

Figs. 3(a) – 3(b) show the Poynting power distribution on the exiting aperture of photoreceptor (S_F), shown in Fig. 2, for different values of Φ, at λ=482nm. As it can be observed, as the incidence angle increases, the forward-scattered power, which represents the power coupled into the outer-segment, decreases. Further, the peak of the scattered power will shift to the lateral side of the outer-segment. Consequently, negligible power will be available to the rhodopsin (chemical in photoreceptors responsible for the photo-chemical process) to trigger its visual cycle. This result agrees with the observations on the directional sensitivity in human vision.

To investigate the total power available to the rhodopsin molecules, we integrate the forward-scattered power over the S_F surface (Fig. 2) for the complete range of visible wavelengths. Figs. 4 show the spectrum of irradiance scattered power on S_F surface of Fig. 2 for angles of incidence Φ=π/10, Φ= π/12. We see that the value of guided power is higher in the laminar structure, which consists of stacking nano-layers of cytoplasm and membrane. Furthermore, for Φ=π/10 and Φ=π/12, there is a shift of the irradiance power peak towards higher wavelengths in the laminar structure, which can explain the small difference (towards higher wavelengths), between the spectral sensitivity of rhodopsin molecules in intact photoreceptor and their solution [16].

5. Acknowledgments

This research was funded by Natural Science and Engineering Research Council of Canada (NSERC) and ***Le Fonds québécois de la recherche sur la nature et les technologies*** (FQRNT). We are grateful for their support.

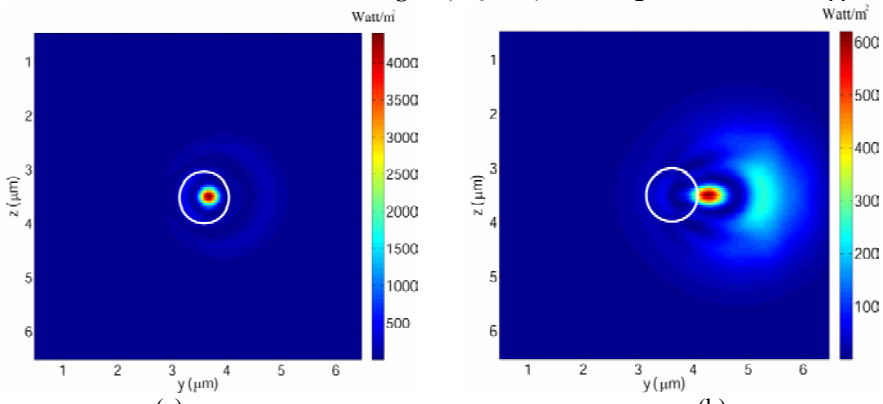

(a) (b)

Fig. 3: The white circle shows the boundary of S_F defined in Fig. 2. Graphs show the Poynting power distribution across surface S_F for two incident angles: a) Φ=π/45, b) Φ=π/12

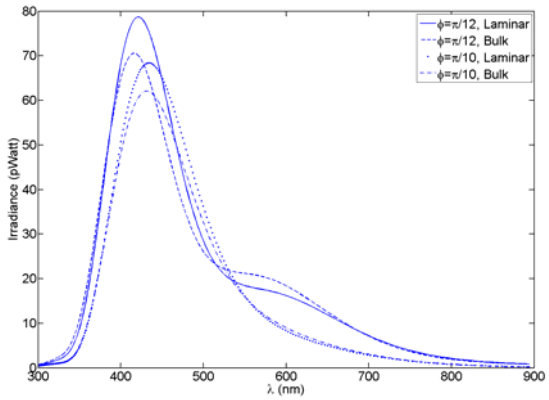

Fig. 4: Irradiance for ψ=π/2, Φ= π /10 and Φ= π /12 for two different structures: one characterized by a bulk averaged refractive index and the other (laminar) by refractive indices of stacking nano-layers of cytoplasm and membrane.

6. References

[1] J. M. Enoch, "Visualization of waveguide modes in retinal receptors," *American Journal of Ophthalmology,* pp. 1107-1118, 1961.

[2] A. W. Snyder and C. Pask, "The Stiles-Crawford effect- explanation and consequences," *Vision Res.,* vol. 13, pp. 1115-1137, 1973.

[3] J. M. Enoch and F. L. T. Jr., *Vertebrate Photoreceptor Optics*: Springer-Verlag Berlin, 1981.

[4] A. C. Guyton, *Text book of Medical Physiology*, 8 ed.: W.B. Saunders Com, 1991.

[5] G. t. D. Francia, "Retina cones as dielectric antennas," *Journal of Optical Society of America,* vol. 39, April 1949.

[6] A. Pozo, F. Perez-Ocon, and J. R. Jimenez, "FDTD analysis of the light propagation in the cones of the human retina: an approach to the Stiles–Crawford effect of the first kind," *Journal Of Optics A: Pure And Applied Optics,* vol. 7, pp. 357–363, 12 July 2005.

[7] M. J. Piket-May and A. Taflove, "Electrodynamics of visible-light interactions with the vertebrate retinal rod," *Optics letters,* vol. 18, April 15, 1993.

[8] A. Hajiaboli and M. Popovic, "Human Retinal Photoreceptors: Electrodynamic Model of Optical Micro-Filters," *To be published in Jan/Feb Issue of IEEE Journal On Selected Topics in Quantum Electronics: Special Issue on Bio-Photonics,* 2008.

[9] A. Hajiaboli and M. Popovic, "FDTD Analysis of Light Propagation in the Human Photoreceptor Cells," *To be published in IEEE Trans. On Magnetics,* vol. 44, 2008.

[10] T. T. J. M. B. Peter J. DeLint, Jan van de Kraats, and Dirk van Norren, "Slow optical changes in human photoreceptors induced by light," *Investigative Ophthalmology & Visual Science,* vol. 41, pp. 282-289, 2000.

[11] F. L. Harosi, "Microspectrophotometry and optical phenomena: Birefringence, dichroism and anamalous dispersion," in *Vertebrate Photoreceptor Optics*, J. M. Enoch and F. L. Tobey, Ed.: Springer-Verlag, 1981, pp. 337-399.

[12] P. A. Liebman, W. S. Jagger, M. W. Kaplan, and F. G. Bargoot, "Membrane structure changes in rod outer segments associated with rhodopsin bleaching," *Nature,* vol. 251, pp. 31-36, 1974.

[13] D. G. Stavenga and H. H. V. Barneveld, "On dispersion in visual photoreceptors," *Vision Res.,* vol. 15, pp. 1091-1095, 1975.

[14] A. Taflove and S. C. Hagness, *Computational Electrodynamics: The Finite-Difference Time-Domain Method*: Artech House, 2005.

[15] A. Fein and E. Z. Szuts, *Photoreceptors: Their Role in Vision*: Cambridge University Press, 1982.

[16] P. A. Liebman, "In situ microspectrophotometric studies on the pigments of single retinal rods," *Biophysical Jornal,* vol. 2, pp. 162-178, 1962.